ResearchGate

See discussions, stats, and author profiles for this publication at: https://www.researchgate.net/publication/263895962

Solution and Solid-State Photoreductive Elimination of Chlorine by Irradiation of a [PtSb] (VII) Complex

ARTICLE *in* JOURNAL OF THE AMERICAN CHEMICAL SOCIETY · JULY 2014

Impact Factor: 12.11 · DOI: 10.1021/ja5056164 · Source: PubMed

CITATIONS
10

READS
11

2 AUTHORS, INCLUDING:

Haifeng Yang
Texas A&M University
4 PUBLICATIONS **13** CITATIONS

SEE PROFILE

Available from: Haifeng Yang
Retrieved on: 28 January 2016

JACS
JOURNAL OF THE AMERICAN CHEMICAL SOCIETY
Communication
pubs.acs.org/JACS

Solution and Solid-State Photoreductive Elimination of Chlorine by Irradiation of a $[PtSb]^{VII}$ Complex

Haifeng Yang and François P. Gabbaï*

Department of Chemistry, Texas A&M University, College Station, Texas 77843, United States

Supporting Information

ABSTRACT: In our search for novel main-group-based redox-active platforms for solar fuel production, we have synthesized $Cl_2Sb^{IV}Pt^{III}Cl_3(o\text{-dppp})_2$ (**2**, *o*-dppp = *o*-$(Ph_2P)C_6H_4$)), a complex featuring a highly oxidized $[PtSb]^{VII}$ core. This thermally stable complex quickly evolves chlorine upon irradiation with a Xe lamp, leading to $[Cl_2Sb^{IV}Pt^{I}Cl(o\text{-dppp})_2]$ (**1**) as the photoproduct. This photoreduction is very efficient, with a maximum quantum yield of 13.8% when carried out in a 4.4 M solution of 2,3-dimethyl-1,3-butadiene in CH_2Cl_2. Remarkably, **2** also evolves chlorine when irradiated in the solid state under ambient conditions in the absence of a trap.

The photoreductive elimination of halogens from transition metal complexes is a thermodynamically difficult process which necessitates the activation of strong metal−halide bonds. Given the relevance of such reactions to the photoinduced splitting of hydrohalic acids,[1] a great deal of effort has been devoted to identifying molecular platforms that support such transformations.[2] Most platforms identified to date contain a late transition metal such as platinum,[2d] iridium,[2e] or gold.[2e] These systems can be mononuclear, as in the case of *trans*-$Pt(PEt_3)_2(Br)_3Ar$ (**A**, Ar = *o*-$(CF_3)C_6H_4$, Chart 1), which

Chart 1

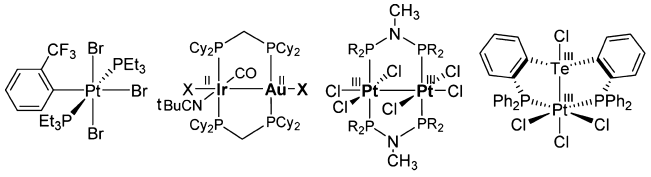

eliminates bromine with a very high quantum yield (Φ) of 82%.[3] Chlorine photoelimination has also been actively pursued because of its relevance to HCl splitting. Two of the best platforms reported to date for chlorine elimination are the Au^{II}−Ir^{II} complex **B** (maximum Φ = 10%, Chart 1)[2e] and the Pt^{III}−Pt^{III} complex **C** (maximum Φ = 38%, Chart 1).[2d] A common design element uniting these different systems is the use of electron-withdrawing ligands which destabilize the high-valent metal centers, thus favoring reductive elimination.

In a recent paper, we showed that the heterobimetallic Te^{III}−Pt^{III} complex **D** (Chart 1) supports the photoreductive elimination of chlorine with a maximum quantum yield of 4.4%.[4] Although the quantum yield of this reaction is relatively low, these results suggest that poorly exploited heavy main-group elements could be considered in lieu of noble metals.[5]

On the basis of these considerations, we have now chosen to broaden the scope of our approach by testing the use of antimony. Our choice of this element was prompted by the realization that (i) antimony displays a rich III/V redox chemistry, making it well suited for the targeted application,[6] and (ii) the extra valence of tri- or pentavalent antimony when compared to di- or tetravalent tellurium offers an opportunity for a greater degree of electronic control through the incorporation of an extra ligand. This logic led us to consider $[(o\text{-}(Ph_2P)C_6H_4)_2SbCl]$, a ligand derived from $[(o\text{-}(Ph_2P)C_6H_4)_2Te]$ by replacement of the Te atom by a less-electron-releasing SbCl moiety. This ligand could be accessed by comproportionation of neat $SbCl_3$ and $(o\text{-}(Ph_2P)C_6H_4)_3Sb$ at 100 °C.[6b] Reaction of $[(o\text{-}(Ph_2P)C_6H_4)_2SbCl]$ with $(Et_2S)_2PtCl_2$ afforded complex **1** (Scheme 1). This complex

Scheme 1. Synthesis of 1 and 2

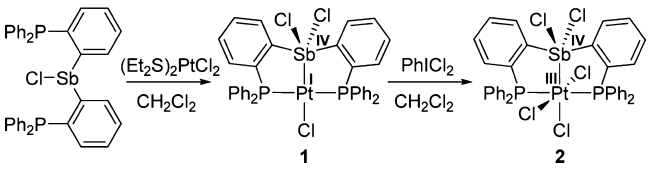

displays a ^{31}P NMR signal at 50.9 ppm and a ^{195}Pt NMR signal at −5164 ppm. The presence of ^{195}Pt satellites in the ^{31}P NMR spectrum and the multiplicity of the ^{195}Pt NMR resonance (triplet, $^1J_{Pt-P}$ = 2566 Hz) confirm the expected coordination of the phosphine arms to the platinum. These spectroscopic features are close to those observed for the stiboranyl complex $[(o\text{-}(Ph_2P)C_6H_4)_2SbClPh]PtCl$ (**E**, $\delta(^{31}P)$ = 53.9 ppm, $\delta(^{195}Pt)$

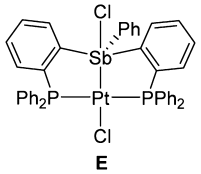

= −5019 ppm, $^1J_{Pt-P}$ = 2706 Hz),[6c] suggesting the possible insertion of the antimony atom into one of the Pt−Cl bonds. This proposal was confirmed by a determination of the crystal structure of **1**, which shows a divalent square-planar platinum

Received: June 4, 2014
Published: July 14, 2014

 © 2014 American Chemical Society dx.doi.org/10.1021/ja5056164 | J. Am. Chem. Soc. 2014, 136, 10866−10869

center with a dichlorodiarylstiboranyl ligand positioned trans from the chloride ligand (Sb–Pt–Cl(3) = 175.25(3)°, P(1)–Pt–P(2) = 169.86(5)°, Figure 1). The Sb–Pt bond of

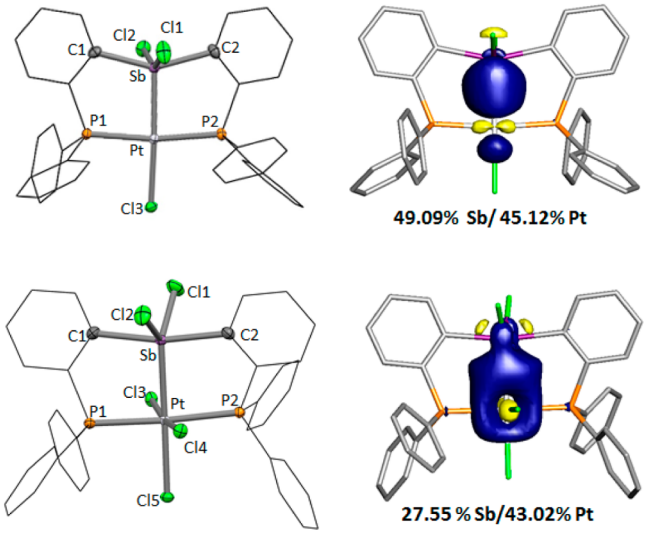

Figure 1. Solid-state structures of **1** (top left) and **2** (bottom left). Thermal ellipsoids are drawn at the 50% probability level. Phenyl groups are drawn in wireframe. Hydrogen atoms are omitted for clarity. Pertinent metric parameters can be found in the text. NLMO plots (isovalue = 0.05) of the Sb–Pt bond in **1** (top right) and **2** (bottom right) obtained from the NBO analysis. Hydrogen atoms are omitted for clarity.

2.4407(5) Å for **1** is notably shorter than that observed in **E** (2.5380(8) Å),[6c] a complex also formed by insertion of the antimony atom into a Pt–Cl bond. The shorter bond observed in **1** most likely originates from the geometry adopted by the pentavalent antimony atom. In **E**, one of the antimony-bound chloride ligands is located directly opposite from the platinum center, thus lengthening the Sb–Pt bond via a trans influence. In **1**, we observe a very different situation, with the two antimony-bound chloride ligands projecting in a direction oblique to the Pt–Sb bond (Pt–Sb–Cl(1) = 99.22(4)°, Pt–Sb–Cl(2) = 107.51(4)°). The coordination geometry at antimony is best described as square pyramidal, with the two chlorine atoms Cl(1) and Cl(2) and the two carbon atoms C(1) and C(2) defining the base (Cl(1)–Sb–Cl(2) = 153.24(5)°, C(1)–Sb–C(2) = 153.7(2)°).

It became important to verify whether **1**, with three electron-withdrawing ligands decorating its core, would be amenable to oxidation. While no reaction was observed with HCl in CH_2Cl_2/Et_2O mixtures, **1** quickly reacted with $PhICl_2$ in CH_2Cl_2 to afford complex **2** as a deep yellow solid. The ^{31}P NMR spectrum of **2** displays a signal at 43.3 ppm with ^{195}Pt satellites ($^1J_{Pt-P}$ = 1842 Hz) as well as a ^{195}Pt NMR resonance at −3473 ppm. When **2** is compared to **1**, its $^1J_{Pt-P}$ coupling constant is notably reduced and its ^{195}Pt NMR resonance is shifted downfield, consistent with oxidation of the platinum center.[7] Although tetravalent platinum complexes are known to thermally eliminate halogens,[3,8] ^{31}P and ^1H NMR spectroscopy shows that **2** remains intact when heated to 70 °C in the solid state for 12 h. The UV–vis spectrum of **2** displays an intense low-energy band centered at 320 nm (ε = 30 005 M^{-1} cm^{-1}), which tails into the visible part of the spectrum (Figure 2). X-ray diffraction confirms Cl_2 addition to the platinum center, which now exhibits an octahedral geometry, with three chloride

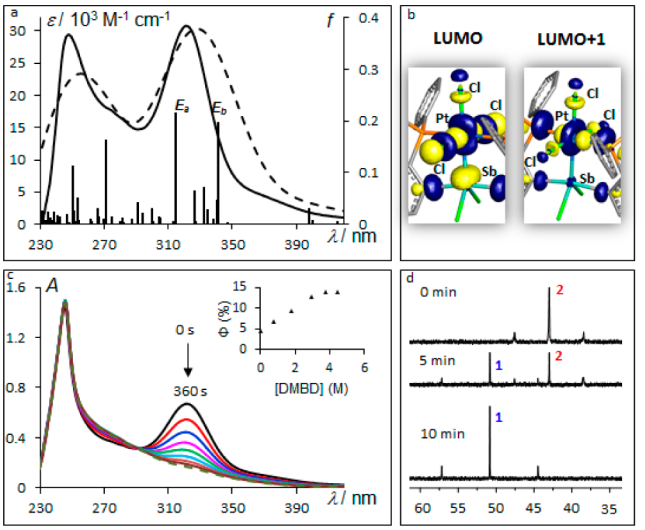

Figure 2. (a) Experimental (CH_2Cl_2, solid line) and calculated (dashed line) ultraviolet–visible spectra for **2**. The calculated spectra were obtained by TD-DFT calculations using the MPW1PW91 functional and a mixed basis set (peak half-width used for the simulation: 0.25 eV). The computed excitations are shown as thin lines with heights proportional to the calculated oscillator strengths. (b) Plots of the LUMO (−0.120 eV) and LUMO+1 (−0.106 eV) of **2** (0.03 isosurface value). (c) Absorption spectra obtained during the photolysis of **2** in CH_2Cl_2 (2.23×10^{-5} M) with monochromatic 320 nm light in the presence of 2,3-dimethyl-1,3-butadiene (7.07×10^{-4} M). The final spectrum is identical to that of **1**. The inset shows the correlation between the quantum yield and the DMBD concentration. (d) ^{31}P NMR spectra of photolysis of **2** in CH_2Cl_2 (0.011 M) in the presence of 2,3-dimethyl-1,3-butadiene (1.77 M).

ligands arranged in a meridional fashion (Figure 1). It is interesting to note that the bond distance of 2.4405(6) Å separating the platinum atom and the chlorine atom (Cl(5)) trans from the antimony atom is longer than the Pt–Cl bond distances involving the chlorine atoms trans from each other (Pt–Cl(2) = 2.3429(5) Å, Pt–Cl(4) = 2.3231(5) Å). This noticeable difference suggests that the antimony ligand is a stronger σ-donor than a chloride ligand. Oxidation of the platinum center also induced some changes at antimony: (i) an important shortening of the Sb–Cl bond from 2.494(3) Å (av.) in **1** to 2.402(2) Å (av.) in **2** and (ii) a contraction of the Cl(1)–Sb–Cl(2) angle from 153.24(5)° in **1** to 118.67(2)° in **2**. As a result, the antimony atom displays a slightly distorted trigonal-bipyramidal geometry, with Cl(1)–Sb–Pt and Cl(2)–Sb–Pt angles of 119.99(2)° and 121.33(2)°, respectively. Finally, the increase in the coordination number of the platinum center is accompanied by a detectable lengthening of the Sb–Pt bond from 2.4407(5) Å in **1** to 2.560(2) Å in **2**.

A Natural Bond Orbital (NBO) analysis of **1** and **2** carried out at the DFT-optimized geometry (Gaussian 09 program; BP86 functional;[9] mixed basis sets: Sb/Pt, cc-pVTZ-PP; P/Cl, 6-31g(d′); and C/H, 6-31g)[10] shows that the Sb–Pt σ-bond is largely covalent for both complexes (see NLMO plots in Figure 1). For **1**, the orbital contributions from antimony and platinum (Sb, 49.09%; Pt, 45.12%) are almost identical, indicating that the bond is essentially nonpolar. Because of the covalent character of this bond and by analogy with formal oxidation state assignments[11] in complexes with metal–metal bonds such as **B** and **C**,[2d,e] we describe **1** as a $Sb^{IV}Pt^{I}$ complex. In **2**, the orbital contributions (Sb, 27.55%; Pt, 43.02%) show

dx.doi.org/10.1021/ja5056164 | J. Am. Chem. Soc. 2014, 136, 10866–10869

that the bonding pair is significantly shifted toward the oxidized and thus more-electron-demanding platinum center. This shift of the bonding density shows that oxidation impacts the core electronic distribution of this heterobimetallic platfom. The polarization of the Sb−Pt bond in **2** is best reconciled by invoking the two resonance structures (**a** and **b**) shown in Chart 2. Resonance structure **a**, which corresponds to a

Chart 2. Relevant Resonance Structures of 2

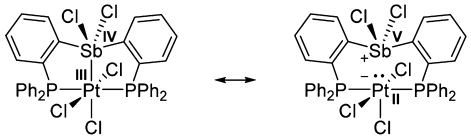

$Sb^{IV}Pt^{III}$ complex, is the most important contributor to the actual electronic structure of the complex. The second resonance structure, **b**, which accounts for the polarization of the Sb−Pt bonding pair toward platinum, corresponds to a platinate (Pt^{II}) complex stabilized by a Z-type or σ-accepting stibonium (Sb^{V}) ligand.[12]

Computational methods have also been used to simulate the UV−vis spectrum of **2** using time-dependent density functional theory (TD-DFT). A good match with the experimental data is obtained when the spectrum is simulated using the MPW1PW91 functional (mixed basis sets: Sb/Pt, cc-pVTZ-PP; P/Cl, 6-31g(d′); C/H, 6-31g) and the SMD implicit solvation model with CH_2Cl_2 as a solvent (Figure 2a).[13] According to these calculations, the high oscillator strength excitations labeled as E_a and E_b contribute to the 320 nm band and involve the LUMO and LUMO+1 as the accepting orbitals. As could be expected for an octahedrally coordinated platinum species, these two orbitals have e_g* character and are antibonding with respect to the Pt−Cl bonds (Figure 2b). In agreement with this spectroscopic assignment, irradiation of **2** in CH_2Cl_2 results in a rapid quenching of the band at 320 nm, suggesting photoreduction of the complex (Scheme 2, Figure

Scheme 2. Photoreduction of 2 Using a Xe Lamp (75 W)[a]

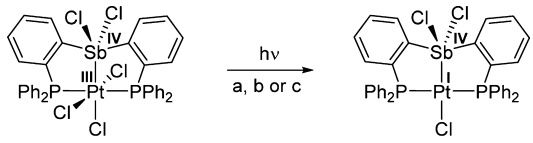

[a]Conditions: (a) solution photolysis in CH_2Cl_2 with DMBD (1.77 M) in a glass NMR tube (complete conversion in 10 min); (b) solid-state photolysis in a closed quartz cell with Na as a trap (conversion = 53% in 10 h); (c) solid-state photolysis in an open quartz cell (conversion = 45% in 10 h).

2c). This photoreduction can be monitored by ^{31}P NMR spectroscopy. When carried out in neat CH_2Cl_2, the reaction affords **1** in ∼85% yield, with some decomposition products detected in the 10−37 ppm range (see SI). The presence of these decomposition products can be assigned to side reactions between the ligand and the chlorine generated by photolysis. As documented in the literature, chlorine atoms can also be trapped by reaction with the CH_2Cl_2 solvent.[14] Addition of 2,3-dimethyl-1,3-butadiene (DMBD, 1.77 M) to the solution as a chlorine scavenger makes the photolysis significantly cleaner, with **1** as the sole phosphorus-containing species (Figure 2d).[2a,c−h] This photoreductive elimination of chlorine is efficient, with a maximum quantum yield of 13.8% measured at a DMBD concentration of 4.4 M, using potassium ferrioxalate as a standard actinometer.[15] The high quantum yield of this photoreductive elimination, which exceeds that of the tellurium complex **D**,[4] is correlated to the destabilizing effect of the five electron-withdrawing chlorine ligands on the oxidized core of **2**. This situation is reminiscent of that described for the hexachlorodiplatinum complex **C**, for which a maximum quantum efficiency of 38% has been reported.[2b] It is also interesting to note that the quantum yield measured for the photoreduction of **2** is comparable to the value of 19% measured for the photoaquation of $[PtCl_6]^{2-}$ (λ = 313 nm), a reaction that proceeds through formation of a Pt(III) intermediate via extrusion of a $Cl^{\bullet}$ radical.[16]

To conclude these studies, we decided to test whether **2** would behave like **C** and evolve chlorine in the solid state.[2d] To this end, a sample of **2** was loaded into a quartz cell at atmospheric pressure, under nitrogen. A small sodium strip, whose base was covered with Teflon tape in order to prevent contact with **2**, was placed inside the cell. The cell was tightly closed and irradiated with a Xe lamp for 10 h (Scheme 2). The temperature of the sample, which was monitored with a mercury thermometer directly adjoining the cell, was kept below 32 °C using a high-velocity fan during photolysis. After 10 h, the photolysis was stopped. The solid sample showed noticeable signs of discoloration, in agreement with the conversion of deep yellow **2** into pale yellow **1**. The surface of the sodium strip had tarnished significantly, suggesting chlorine oxidation. In line with these observations, ^{1}H and ^{31}P NMR analysis of the photolyzed solid indicated a 53% conversion of **2** into **1**. The evolution of chlorine was confirmed by dissolution of the sodium strip in water and subsequent chloride analysis using ion chromatography. The latter indicated that 72% of the expected chlorine had been captured by sodium during the photolysis experiment. We propose that the rest of the chlorine is incorporated in the decomposition products observed by ^{31}P NMR spectroscopy in the 5−25 ppm range (see SI). Using single-point energy calculations carried out with the B3LYP functional and a mixed basis set (C/H/P/Cl, 6-311+g(2d,p); Sb/Pt, cc-pVTZ-PP), we estimate that the photoreduction of **2** into **1** is endothermic by 544 kJ/mol, assuming the formation of two $Cl^{\bullet}$ radicals, or by 300 kJ/mol, assuming the formation of Cl_2. These values provide a measure of the energy-storing potential of this reaction. Finally, the solid-state photolysis of **2** into **1** can be carried out with the cell open to air without sodium as a chemical trap (Figure 3, conversion of 45% after 10 h). The evolution of chlorine under such conditions shows that the title SbPt complex is able to evolve chlorine on its own, without the thermodynamic bias associated with a trap. To our knowledge, no other bimetallic complexes have been tested under such conditions. Complex **C** also evolves chlorine when irradiated in the solid state, albeit under vacuum, with the chlorine photoproduct captured in a low-temperature trap.[2d]

In summary, we describe a new SbPt platform for the high-quantum-yield photoevolution of chlorine. The photoreduction quantum yield of **2** is more than 3 times greater than that measured for the TePt complex **D** previously investigated by our group.[4] This increase supports the notion that replacement of the TeCl unit in **D** by a less-electron-releasing $SbCl_2$ unit in **2** destabilizes the oxidized complex and facilitates its photo-

dx.doi.org/10.1021/ja5056164 | J. Am. Chem. Soc. 2014, 136, 10866−10869

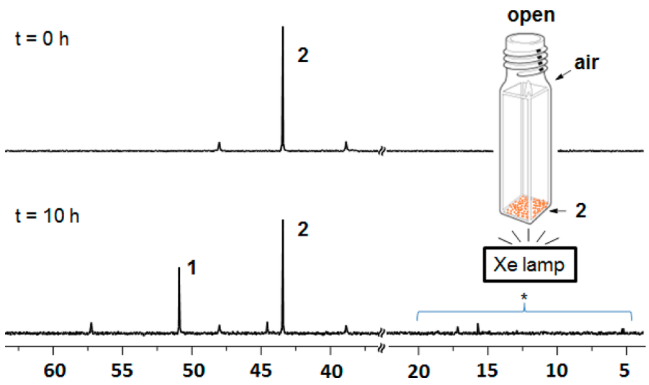

Figure 3. ^{31}P NMR spectra before and after solid-state irradiation of **2** with a Xe lamp (75 W) under ambient conditions in an open quartz cell. The inset shows a schematic drawing of the experimental setup used for this open-system solid-state photolysis. The spectral region marked by an asterisk shows the presence of decomposition products.

reduction. Another unique feature of the title SbPt platform is its ability to support this reaction in the solid state, in the absence of a trap. We propose that such platforms may become useful for the production of halogens as solar fuels. We are currently investigating the mechanism of this solid-state reaction and whether chlorine is evolved as $Cl^{\bullet}$ or Cl_2.[17]

■ ASSOCIATED CONTENT

Supporting Information

Additional experimental and computational details; crystallographic data in CIF format. This material is available free of charge via the Internet at http://pubs.acs.org.

■ AUTHOR INFORMATION

Corresponding Author

francois@tamu.edu

Notes

The authors declare no competing financial interest.

■ ACKNOWLEDGMENTS

This work was supported by the National Science Foundation (CHE-1300371), the Welch Foundation (A-1423), and Texas A&M University (Arthur E. Martell Chair of Chemistry).

■ REFERENCES

(1) (a) Mann, K. R.; Lewis, N. S.; Miskowski, V. M.; Erwin, D. K.; Hammond, G. S.; Gray, H. B. *J. Am. Chem. Soc.* **1977**, *99*, 5525−5526. (b) Mann, K. R.; Bell, R. A.; Gray, H. B. *Inorg. Chem.* **1979**, *18*, 2671−2673. (c) Maverick, A. W.; Gray, H. B. *Pure Appl. Chem.* **1980**, *52*, 2339−2348. (d) Sigal, I. S.; Mann, K. R.; Gray, H. B. *J. Am. Chem. Soc.* **1980**, *102*, 7252−7256. (e) Mann, K. R.; Dipierro, M. J.; Gill, T. P. *J. Am. Chem. Soc.* **1980**, *102*, 3965−3967. (f) Gray, H. B.; Maverick, A. W. *Science* **1981**, *214*, 1201−1205. (g) Eidem, P. K.; Maverick, A. W.; Gray, H. B. *Inorg. Chim. Acta* **1981**, *50*, 59−64. (h) Heyduk, A. F.; Nocera, D. G. *Science* **2001**, *293*, 1639−1641. (i) Esswein, A. J.; Nocera, D. G. *Chem. Rev.* **2007**, *107*, 4022−4047.

(2) (a) Heyduk, A. F.; Macintosh, A. M.; Nocera, D. G. *J. Am. Chem. Soc.* **1999**, *121*, 5023−5032. (b) Cook, T. R.; Esswein, A. J.; Nocera, D. G. *J. Am. Chem. Soc.* **2007**, *129*, 10094−10095. (c) Teets, T. S.; Nocera, D. G. *J. Am. Chem. Soc.* **2009**, *131*, 7411−7420. (d) Cook, T. R.; Surendranath, Y.; Nocera, D. G. *J. Am. Chem. Soc.* **2009**, *131*, 28−29. (e) Teets, T. S.; Lutterman, D. A.; Nocera, D. G. *Inorg. Chem.* **2010**, *49*, 3035−3043. (f) Teets, T. S.; Neumann, M. P.; Nocera, D. G. *Chem. Commun.* **2011**, *47*, 1485−1487. (g) Teets, T. S.; Cook, T. R.; McCarthy, B. D.; Nocera, D. G. *Inorg. Chem.* **2011**, *50*, 5223−5233. (h) Cook, T. R.; McCarthy, B. D.; Lutterman, D. A.; Nocera, D. G. *Inorg. Chem.* **2012**, *51*, 5152−5163. (i) Powers, D. C.; Chambers, M. B.; Teets, T. S.; Elgrishi, N.; Anderson, B. L.; Nocera, D. G. *Chem. Sci.* **2013**, *4*, 2880−2885. (j) Wickramasinghe, L. A.; Sharp, P. R. *Inorg. Chem.* **2014**, *53*, 1430−1442.

(3) Karikachery, A. R.; Lee, H. B.; Masjedi, M.; Ross, A.; Moody, M. A.; Cai, X.; Chui, M.; Hoff, C. D.; Sharp, P. R. *Inorg. Chem.* **2013**, *52*, 4113−4119.

(4) Lin, T.-P.; Gabbaï, F. P. *J. Am. Chem. Soc.* **2012**, *134*, 12230−12238.

(5) Carrera, E. I.; McCormick, T. M.; Kapp, M. J.; Lough, A. J.; Seferos, D. S. *Inorg. Chem.* **2013**, *52*, 13779−13790.

(6) (a) Wade, C. R.; Gabbaï, F. P. *Angew. Chem., Int. Ed.* **2011**, *50*, 7369−7372. (b) Ke, I.-S.; Gabbaï, F. P. *Inorg. Chem.* **2013**, *52*, 7145−7151. (c) Ke, I.-S.; Jones, J. S.; Gabbaï, F. P. *Angew. Chem., Int. Ed.* **2014**, *53*, 2633−2637.

(7) (a) Oberhauser, W.; Bachmann, C.; Stampfl, T.; Brüggeller, P. *Inorg. Chim. Acta* **1997**, *256*, 223−234. (b) Oberhauser, W.; Stampfl, T.; Bachmann, C.; Haid, R.; Langes, C.; Kopacka, H.; Ongania, K.-H.; Brüggeller, P. *Polyhedron* **2000**, *19*, 913−923.

(8) (a) Elding, L. I.; Gustafson, L. *Inorg. Chim. Acta* **1976**, *19*, 165−171. (b) Bondarenko, V. S.; Korniets, E. D.; Sokolenko, V. A.; Kovrova, N. B.; Kovtonyuk, N. P. *Zh. Neorg. Khim.* **1989**, *34*, 1541−1543. (c) Bryan, S. A.; Dickson, M. K.; Roundhill, D. M. *Inorg. Chem.* **1987**, *26*, 3878−3886. (d) Levy, C. J.; Puddephatt, R. J. *J. Am. Chem. Soc.* **1997**, *119*, 10127−10136.

(9) (a) Perdew, J. P. *Phys. Rev. B* **1986**, *33*, 8822−8824. (b) Becke, A. D. *Phys. Rev. A* **1988**, *38*, 3098−3100.

(10) (a) Peterson, K. A.; Figgen, D.; Goll, E.; Stoll, H.; Dolg, M. *J. Chem. Phys.* **2003**, *119*, 11113−11123. (b) Figgen, D.; Peterson, K. A.; Dolg, M.; Stoll, H. *J. Chem. Phys.* **2009**, *130*, 164108−164112.

(11) Parkin, G. *J. Chem. Educ.* **2006**, *83*, 791−799.

(12) (a) Shriver, D. F. *Acc. Chem. Res.* **1970**, *3*, 231−238. (b) Dammann, C. B.; Hughey, J. L.; Jicha, D. C.; Meyer, T. J.; Rakita, P. E.; Weaver, T. R. *Inorg. Chem.* **1973**, *12*, 2206−2209. (c) Chan, D. M. T.; Marder, T. B. *Angew. Chem., Int. Ed.* **1988**, *27*, 442−443. (d) Parkin, G. *Organometallics* **2006**, *25*, 4744−4747. (e) Hill, A. F. *Organometallics* **2006**, *25*, 4741−4743. (f) Fontaine, F.-G.; Boudreau, J.; Thibault, M.-H. *Eur. J. Inorg. Chem.* **2008**, *2008*, 5439−5454. (g) Braunschweig, H.; Dewhurst, R. D.; Schneider, A. *Chem. Rev.* **2010**, *110*, 3924−3957. (h) Bouhadir, G.; Amgoune, A.; Bourissou, D. *Adv. Organomet. Chem.* **2010**, *58*, 1−107. (i) Amgoune, A.; Bourissou, D. *Chem. Commun.* **2011**, *47*, 859−871. (j) Braunschweig, H.; Dewhurst, R. D. *Dalton Trans.* **2011**, *40*, 549−558. (k) Bauer, J.; Braunschweig, H.; Dewhurst, R. D. *Chem. Rev.* **2012**, *112*, 4329−4346. (l) Owen, G. R. *Chem. Soc. Rev.* **2012**, *41*, 3535−3546. (m) Kameo, H.; Nakazawa, H. *Chem.—Asian J.* **2013**, *8*, 1720−1734. (n) Mingos, D. M. P. *J. Organomet. Chem.* **2014**, *751*, 153−173.

(13) Marenich, A. V.; Cramer, C. J.; Truhlar, D. G. *J. Phys. Chem. B* **2009**, *113*, 6378−6396.

(14) Alfassi, Z. B.; Mosseri, S.; Neta, P. *J. Phys. Chem.* **1989**, *93*, 1380−1385.

(15) (a) Hatchard, C. G.; Parker, C. A. *Proc. R. Soc. London, Ser. A* **1956**, *235*, 518−536. (b) Parker, C. A. *Proc. R. Soc. London, Ser. A* **1953**, *220*, 104−116. (c) Kuhn, H. J.; Braslavsky, S. E.; Schmidt, R. *Pure Appl. Chem.* **2004**, *76*, 2105−2146.

(16) Znakovskaya, I. V.; Sosedova, Y. A.; Glebov, E. M.; Grivin, V. P.; Plyusnin, V. F. *Photochem. Photobiol. Sci.* **2005**, *4*, 897−902.

(17) Perera, T. A.; Masjedi, M.; Sharp, P. R. *Inorg. Chem.* **2014**, *53*, 7608−7621.